

Temperature-Dependent Photoselection—Intramolecular Exciton Motion in $[\text{Ru}(\text{bpy})_3]^{2+}$

Clifford M. Carlin* and M. Keith DeArmond

Contribution from the Department of Chemistry, North Carolina State University, Raleigh, North Carolina 27695-8204. Received December 19, 1983

Abstract: The investigation of the emitting and other excited states of tris(diimine) chelates of ruthenium(II) has led to a debate over the true molecular symmetry of these species. Although the spectroscopic evidence clearly indicates that the symmetry of these complexes can be lower than D_3 , whether the symmetry reduction is due to solvent-induced distortions in the ground state or to the existence of single-ligand localized excited states has not been unquestionably demonstrated. We have obtained temperature- and solvent-dependent photoselection data in an attempt to verify the existence of single-ligand exciton localization for $[\text{Ru}(\text{bpy})_3]^{2+}$ and $[\text{Ru}(\text{phen})_3]^{2+}$. These data indicate that both intermolecular (solvent-solute) and intramolecular (ligand localization) mechanisms are active in these systems.

Over the past decade an intense interest in the photophysical and photochemical behavior of $[\text{Ru}(\text{bpy})_3]^{2+}$ (bpy = 2,2'-bipyridine) and related complexes has been stimulated by these compounds' unique luminescence properties and their ability to serve as photosensitizers in various redox and solar energy conversion processes.¹⁻⁶ But despite the successful exploitation of the photochemical properties of these molecules, a widely accepted and detailed description of the lowest lying excited states of $[\text{Ru}(\text{bpy})_3]^{2+}$, etc., is not available. The proposal of an electron-ion coupling (EIC) model by Crosby^{7,8} is the most elaborate attempt to describe the luminescing state as well as other, higher energy charge-transfer states. The EIC model presumes strong spin-orbit and interligand coupling, and it is these points and the resultant symmetry assignments at 77 K that have been recently contested. In particular, a considerable mass of data has accumulated which supports the hypothesis that the excited state has a symmetry lower than the D_3 presumed by the EIC model.⁹⁻¹⁴ Although such a symmetry lowering could conceivably be due to environmental factors⁹ some of these data suggest that the symmetry reduction is an intramolecular phenomenon.¹⁰⁻¹³ The results of time-resolved resonance Raman studies of Dallinger and Woodruff¹⁰ and the observed solvent dependence¹¹ of the strong charge-transfer absorption band of $[\text{Ru}(\text{bpy})_3]^{2+}$, etc., are interpreted in terms of single-ligand excited states. Ferguson and Herren¹² have obtained spectroscopic data which suggest that singlet charge-transfer states are delocalized while the triplets may exhibit a more localized character. Additionally, the reexamination by Baggott et al.¹³ of the evidence reported by Crosby and Elfring¹⁵ in support of strong interligand coupling in mixed diimine chelates of Ru(II) has raised some questions about the actual magnitude of the ligand-ligand interactions in these molecules.

With the possible exception of a portion of the work of Baggott, there are not kinetic studies available in the literature to support (or refute) the concept of a single-ligand localized state in $[\text{Ru}(\text{bpy})_3]^{2+}$. The photoselection data previously published by this lab¹⁴ support this hypothesis, but the distinction between environmental (intermolecular) and intramolecular symmetry reduction mechanisms was difficult to demonstrate. Temperature- and solvent-dependent photoselection data have now been obtained to verify the existence of single-ligand localized luminescing state(s) for $[\text{Ru}(\text{bpy})_3]^{2+}$ and $[\text{Ru}(\text{phen})_3]^{2+}$ (phen = 1,10-phenanthroline).

Theory

The theory of time-dependent photoselection spectroscopy has been developed primarily to investigate the rotational dynamics of fluorescing species in relatively low viscosity solvents. Tao¹⁶ has derived the expression for the time-dependent depolarization ratios ($r(t)$) of a general rotor. For a molecule with D_3 symmetry

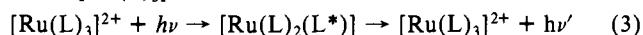
$$r(t) = \frac{1}{5}(3 \cos^2 \lambda - 1) \left[\frac{1}{4} e^{-6D_{\perp}t} + \frac{3}{4} e^{-(2D_{\perp} + 4D_{\parallel})t} \right] \quad (1)$$

where D_{\perp} and D_{\parallel} are rotational "diffusion constants" about the minor and major (C_3) rotation axes and λ is the average angular separation of the absorption and emission oscillators. The depolarization ratio is related to the photoselection polarization,¹⁷ P , by

$$r = 2P/(3 - P) \quad (2)$$

In general the time-dependent and steady-state depolarization ratios will be described by much simpler expressions than the polarization.

Previously reported photoselection data for tris(diimine) complexes of Ru(II) and related compounds suggest that the emission oscillator for these species is linear and perpendicular to the nominally C_3 rotation axis, i.e., it lies along the metal-to-metal ligand axis. If this symmetry reduction is due to the localization of the $[\text{Ru}(\text{L})_3]^{2+}$ excited state, i.e., if



is a valid description of the absorption/emission processes, then it might be expected that at temperatures sufficiently above 77 K the excitation, or exciton, would be transferred between ligands. If this transfer or exciton hopping is described by the first-order hopping rate constant k_h , then the depolarization ratio (eq 1) becomes

$$r(t) = \frac{1}{10(a + b + c)} [(a + b - 2c)e^{-6D_{\perp}t} + 3(a - b)e^{-(2D_{\perp} + 4D_{\parallel} + (3/2)k_h)t}] \quad (4)$$

where the orientation absorption oscillator is described by the vector \hat{A} .

$$\hat{A} = a\hat{x} + b\hat{y} + c\hat{z} \quad (5)$$

- (1) Ghosh, P. K.; Spiro, T. G. *J. Am. Chem. Soc.* **1980**, *102*, 5543.
- (2) Lehn, J. M.; Sauvage, J. P. *Nouv. J. Chem.* **1977**, *1*, 449.
- (3) Kiwi, J.; Gratzel, M. *Angew. Chem., Int. Ed. Engl.* **1979**, *18*, 624.
- (4) Borgarello, E.; Kiwi, J.; Pelizzetti, E.; Visca, M.; Gratzel, M. *Nature (London)* **1980**, *289*, 158.
- (5) Borgarello, E.; Kiwi, J.; Pelizzetti, E.; Visca, M.; Gratzel, M. *J. Am. Chem. Soc.* **1981**, *103*, 6324.
- (6) Kalyanasundaram, K.; Gratzel, M. *Angew. Chem., Int. Ed. Engl.* **1979**, *18*, 701.
- (7) Hipps, K. W.; Crosby, G. A. *J. Am. Chem. Soc.* **1975**, *97*, 7042.
- (8) Harrigan, R. W.; Crosby, G. A. *J. Chem. Phys.* **1973**, *59*, 3468.
- (9) Felix, F.; Ferguson, J.; Gudel, H.; Ludi, A. *J. Am. Chem. Soc.* **1980**, *102*, 4096.
- (10) Dallinger, R. F.; Woodruff, W. H. *J. Am. Chem. Soc.* **1979**, *101*, 4391.
- (11) Meyer, T. J. *Inorg. Chem.*, in press.
- (12) Ferguson, J.; Herren, F. *Chem. Phys. Lett.* **1982**, *89*, 371.
- (13) Baggott, J. E.; et al. *J. Chem. Soc., Faraday Trans. 2* **1983**, *79*, 195.
- (14) Carlin, C. M.; DeArmond, M. K. *Chem. Phys. Lett.* **1982**, *89*, 297.
- (15) Crosby, G. A.; Elfring, W. H., Jr. *J. Phys. Chem.* **1976**, *80*, 2206.
- (16) Tao, T. *Biopolymers* **1969**, *8*, 609.
- (17) Albrecht, A. C. *J. Mol. Spectrosc.* **1961**, *6*, 84.

* Present address: Chemistry Department, University of Maine, Orono, ME 06649.

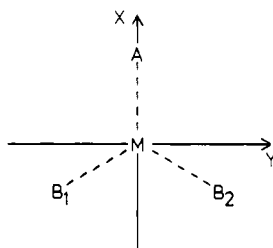


Figure 1. Internal coordinate and ligand labeling scheme for the tris(diimine) chelates.

The coordinate system for eq 4 and 5 is described by Figure 1, in which the x axis is chosen to lie along the metal-to-ligand axis of the initially excited ligand. For $k_h = 0$, eq 4 reduces to eq 1 for the type of emission oscillator described above.

From eq 1 and 4 it is obvious that exciton transfer should not be distinguishable from rotational diffusion about the z molecular axis, since a plot of r vs. time is a dual exponential with lifetimes $6D_{\perp}$ and $2D_{\perp} + 4D_{\parallel} + (3/2)k_h$. However, since $[\text{Ru}(\text{L})_3]^{2+}$ is a molecule with nearly spherical symmetry, eq 4 reduces to

$$r(t) = \frac{1}{10(a + b + c)} [(a + b - 2c)e^{-6D_R t} + 3(a - b)e^{-(6D_R + (3/2)k_h)t}] \quad (6)$$

where

$$D_R = D_{\perp} = D_{\parallel} \quad (7)$$

It is apparent that analysis of the decay characteristics of $r(t)$ described by eq 6 may lead to a determination of k_h .

We did not have the instrumental capability to obtain $r(t)$ at the necessary wavelengths at sufficiently short times to directly apply eq 6. However, with information about the relative magnitudes of a , b , and c at various excitation wavelengths, k_h may be extracted by an analysis of steady-state photoselection polarization spectra at different temperatures. The steady-state expression for r may be obtained from (6) and is

$$r_s = \frac{k_r}{10(a + b + c)} \left[\frac{(a + b - 2c)}{k_r + 6D_R} + \frac{3(a - b)}{k_r + 6D_R + (3/2)k_h} \right] \quad (8)$$

where k_r is the observed radiative rate constant of the emitting state(s). Values of a , b , and c have been obtained¹⁴ from doped single-crystal polarization spectra which are available in the literature.⁹ The k_r is measurable, and if D_R is known or known to be insignificant, k_h may be obtained from eq 8.

It should be noted that depolarization mechanisms not considered in the above derivations will affect experimentally determined values of k_h . Therefore, a nonzero k_h cannot, without additional evidence, be interpreted to suggest that interligand exciton transfer is occurring.

Experimental Section

Materials. $[\text{Ru}(\text{bpy})_3]\text{Cl}_2$ and $[\text{Ru}(\text{phen})_3]\text{Cl}_2$ were prepared by literature methods and purified by cation-exchange chromatography on Cellex-P (Bio-Rad Laboratories). The perchlorate salts were prepared by metathesis with NaClO_4 . This procedure apparently led to the coprecipitation of $[\text{Ru}(\text{bpy})_3](\text{ClO}_4)_2$ and NaClO_4 . Expected for $[\text{Ru}(\text{bpy})_3](\text{ClO}_4)_2 \cdot 2\text{H}_2\text{O} \cdot 3\text{NaClO}_4$: C, 30.7%; H, 2.41%; N, 7.17%; Cl, 15.1%. Found: C, 30.3%; H, 2.70%; N, 7.00%; Cl, 15.0%. This was not a problem with $[\text{Ru}(\text{phen})_3](\text{ClO}_4)_2$ and a very good analysis was obtained. Expected for $[\text{Ru}(\text{phen})_3](\text{ClO}_4)_2 \cdot 4\text{H}_2\text{O}$: C, 47.34%; H, 3.53%; N, 9.50%; Cl, 7.76%. Found: C, 47.41%; H, 3.51%; N, 9.21%; Cl, 7.71%. All analyses were performed by Galbraith Laboratories.

All solvents were nonluminescent in the spectral regions employed.

Instrumentation. The photoselection spectrometer used in this study has been described elsewhere.¹⁸ For variable temperature work, the glassy samples were contained in sealed glass tubes (4-mm o.d.) which were inserted into a 4–5 mm i.d. copper tube. The copper tube served as a sample holder in conjunction with an Air Products WMX-15 EPR vacuum shroud. Temperature was maintained to ± 0.2 K (between 80

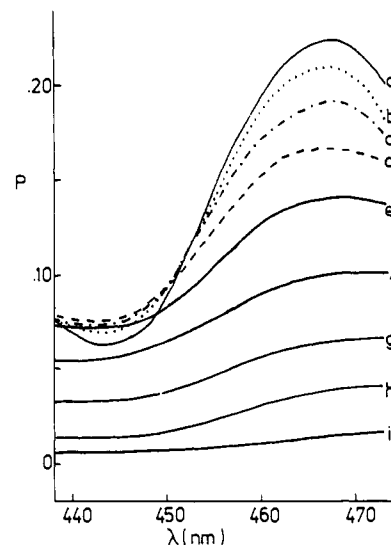


Figure 2. Excitation photoselection spectra of $[\text{Ru}(\text{bpy})_3]^{2+}$ in 4:1 ethanol/methanol at indicated temperatures; 595-nm emission: (a) average of 90, 95, 100, and 105 K; (b–i) 110–145 K by 5 K increments.

and 300 K) with an Air Products LT-3-110 Cryo-tip liquid-transfer system (used with liquid nitrogen) and an APD-E temperature indicator/controller.

The detailed analysis of the $[\text{Ru}(\text{bpy})_3]^{2+}$ photoselection spectra presented below requires temperature-dependent decay constants. These were determined from relative integrated emission intensities in glycerin and 4:1 ethanol/methanol and from single-temperature experimental lifetimes by

$$k_r(T) = \frac{I(T)}{I(T')\tau(T')} \quad (9)$$

where $k_r(T)$ and $I(T)$ are the observed decay constant and integrated emission intensity at temperature T and $I(T')$ are the observed decay constant and integrated emission intensity at temperature T' and $\tau(T')$ are the integrated emission intensity and measured lifetime at temperature T' . The emission intensities were obtained by setting the excitation and emission monochromators to 0 nm and using the spectrometer as a filter fluorometer to obtain "integrated" emission intensities.

Results

Temperature-dependent excitation photoselection spectra for $[\text{Ru}(\text{bpy})_3]^{2+}$ in 4:1 ethanol/methanol, 3:2 methanol/water, 1:1 ethylene glycol/water and glycerin appear in Figures 2–5. The uncertainties associated with the polarization data reported in these figures are estimated to be less than 0.002 for spectra having high P values and 0.01 for low polarizations.

There are several interesting features associated with the spectra in Figures 2–5. Most obviously there is a temperature at which depolarization processes become apparent (110 K in ethanol/methanol, 160–170 K in ethylene glycol/water, and 190–200 K in glycerin), above which depolarization progresses until P becomes nearly zero at all wavelengths. The methanol/water solution became turbid at 140 K, so completely polarized spectra could not be obtained. The photoselection spectra are nearly flat in glycerin at 260 K ($P \sim 0.09$) and in ethylene glycol/water at 210 K ($P \sim 0.03$). The ethanol/methanol spectra depolarize, but after an initial phase of "flattening" between 110 and 120 K, the photoselection spectrum depolarizes at a fairly uniform rate for all wavelengths. Based on data over the limited temperature range for methanol/water, spectra for this solvent have behavior intermediate between the glycerin and mixed alcohol spectra.

Temperature-dependent photoselection spectra for $[\text{Ru}(\text{phen})_3]^{2+}$ in 4:1 ethanol/methanol and glycerin appear in Figures 6 and 7. The features of these spectra and their temperature dependence are similar to those of $[\text{Ru}(\text{bpy})_3]^{2+}$ in Figures 2 and 5.

Discussion

The photoselection spectra presented in Figures 2–7 exhibit temperature dependences which appear to be a function of solvent

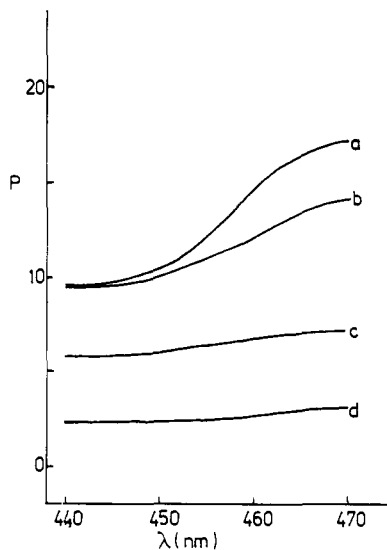


Figure 3. Excitation photoselection spectra for $[\text{Ru}(\text{bpy})_3]^{2+}$ in 3:2 (w/w) methanol/water at indicated temperatures: 580-nm emission; (a-d) 150–180 K by 10 K increments.

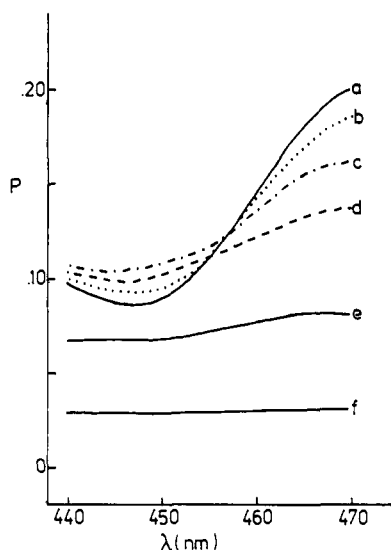


Figure 4. Excitation photoselection spectra for $[\text{Ru}(\text{bpy})_3]^{2+}$ in 1:1 (v/v) ethylene glycol/water at indicated temperatures: 580-nm emission; (a-f) 160–210 K by 10 K increments.

melting point. In the case of glycerin, both the $[\text{Ru}(\text{bpy})_3]^{2+}$ and $[\text{Ru}(\text{phen})_3]^{2+}$ excitation photoselection spectra become nearly flat ($P \sim 0.09$ at all wavelengths) well before complete depolarization ($P = 0.00$). For the lower melting point ethanol/methanol solutions, the structure of the photoselection spectra does not appear to be lost until, at sufficiently high temperatures, decreasing solvent viscosity leads to a complete loss of polarization information. The behaviors of the methanol/water and ethylene glycol/water spectra for $[\text{Ru}(\text{bpy})_3]^{2+}$ may be considered to fall between those of the other two solvents.

That the temperature dependence of these photoselection spectra may provide insight into the depolarizing mechanism is illustrated in Figure 8. In this figure, either D_R or k_h is assumed to be increasing with temperature while the other is small (zero). Under these conditions, r_s (eq 8), and therefore P , can be seen to be a function only of the ratio D_R/k_r or k_h/k_r . If k_r is assumed to be nearly independent of temperature, these ratios would be expected to increase with temperature. As might be expected, increases in k_h (Figure 8A) lead to a flattening of the photoselection spectra as x and y are made equivalent (planar depolarization) by either the transfer of the excited state between ligands in the x - y molecular plane or relaxation of a solvent-induced distortion. For spherical rotational depolarization (Figure 8B), increasing D_R

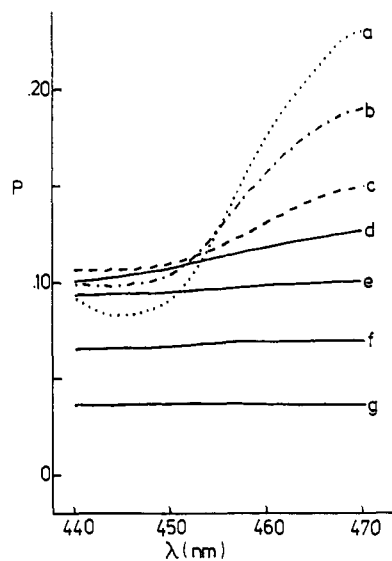


Figure 5. Excitation photoselection spectra of $[\text{Ru}(\text{bpy})_3]^{2+}$ in glycerin at indicated temperatures: 580-nm emission; (a) 170 K; (b) 220 K; (c-g) 240–280 K by 10 K increments.

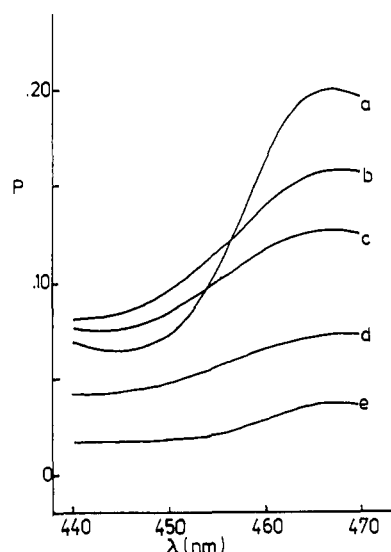


Figure 6. Excitation photoselection spectra of $[\text{Ru}(\text{phen})_3]^{2+}$ in approximately 4:1 (v/v) ethanol/methanol at indicated temperatures: 580-nm emission; (a) 110 K; (b) 120 K; (c) 124 K; (d) 130 K; (e) 140 K.

causes a monotonic decrease in P at all wavelengths such that the basic structure of the spectrum is maintained throughout the depolarization process. In both A and B of Figure 8, as done previously,¹⁴ the absorption oscillator description of Ferguson et al.⁹ from doped crystal data was used to define a , b , and c for the excitation wavelengths shown.

Comparison of Figure 8 with Figures 2–7 suggests that at least two depolarization mechanisms must be considered to explain the observed photoselection spectra. In the high-melting glycerin solution, $[\text{Ru}(\text{bpy})_3]^{2+}$ and $[\text{Ru}(\text{phen})_3]^{2+}$ clearly exhibit depolarization in the x - y plane (planar depolarization) which is nearly complete by 260 K. At that temperature, involvement of the z molecular axis is becoming important so that complete depolarization effectively occurs by about 300 K. Alone, the glycerin data cannot be used to distinguish between intramolecular exciton localization or solvent-solute interactions (ground-state distortion), since a solvent-induced distortion might be active only at high viscosities. However, the data for the mixed alcohol solvent (Figures 2 and 6) argue against the latter, since it is apparent that in ethanol/methanol a high degree of x - y distinguishability is retained (the photoselection spectra retain their structure) as spherical rotational depolarization is becoming nearly total. It

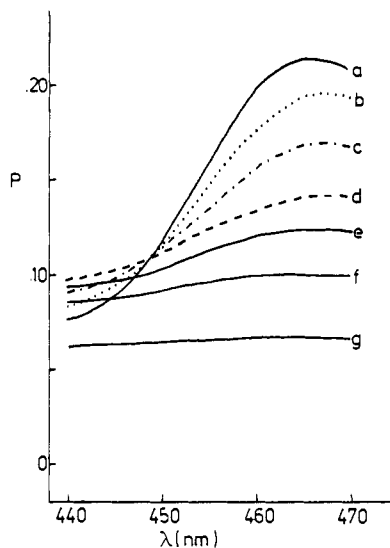


Figure 7. Excitation photoselection spectra of $[\text{Ru}(\text{phen})_3]^{2+}$ in glycerin at indicated temperatures: 565-nm emission; (a) 180 K; (b) 210 K; (c) 225 K; (d) 235 K; (e) 245 K; (f) 250 K; (g) 260 K.

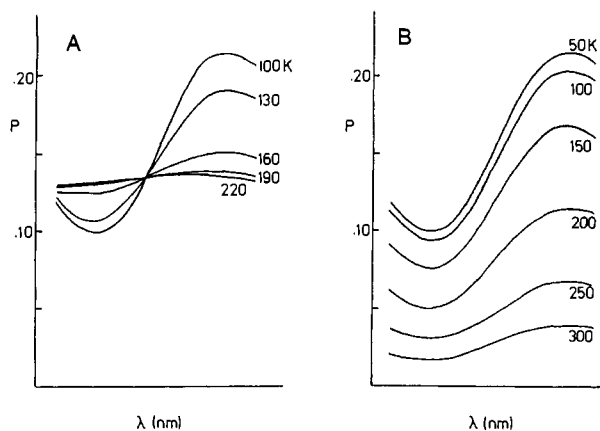


Figure 8. Simulated photoselection spectra in (A) $k_h/k_r = 0$ (a), 0.29 (b), 2.3 (c), 9.7 (d), 2.7 (e) and in (B) $D_R/k_r = 0$ (a), 0.01 (b), 0.68 (c), 2.1 (d), 3.6 (e), 5.0 (f).

seems unlikely that a ground state, intermolecular distortion mechanism could be responsible for the residual x - y splitting in an environment of nearly complete rotational depolarization.

The above considerations prompted an attempt to extract hopping rates from the glycerin data using eq 8. The k_r values were estimated as described. The D_R values were estimated in the temperature range 205–245 K by extrapolation of calculated values from 250 to 280 K. The higher temperature D_R values were calculated by noting that the low-temperature glycerin data for $[\text{Ru}(\text{bpy})_3]^{2+}$ cross at 454 nm. This implies $a \approx b$ at this wavelength, and under this condition (8) simplifies to

$$r_s = \frac{k_r(a-c)}{5(2a+c)(k_r+6D_R)} \quad (10)$$

which, when rearranged, leads to

$$D_R = \frac{k_r}{6} \left[\frac{(a-c)}{5r_s(2a+c)} - 1 \right] \quad (11)$$

Relative a and c are set from the maximum limit of r_s ($D_R \equiv 0$), which from (11) is

$$r_s = \frac{a-c}{5(2a+c)} \quad (12)$$

The D_R values were obtained by (11) for data from Figure 5, 250–280 K. These were fit to the usual temperature expression for D_R

$$D_R = D_R^\circ T/\eta \quad (13)$$

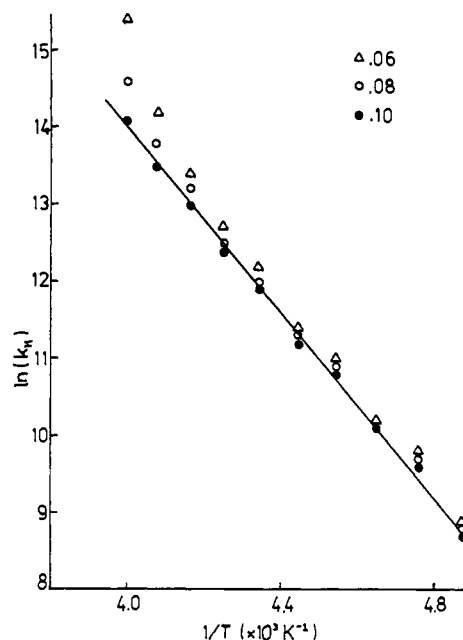


Figure 9. Arrhenius plots of calculated k_h for $[\text{Ru}(\text{bpy})_3]^{2+}$ in glycerol for indicated C' . The line is a least-squares fit to the $C' = 0.10$ data.

in order to obtain D_e° . The D_R at lower temperature was determined from (13) with known¹⁹ or (below 230 K) extrapolated values of η . For temperatures below 230 K, good estimates were not actually required since D_R was rapidly becoming insignificant. The k_h values were then calculated from a rearrangement of eq 8 for the $[\text{Ru}(\text{bpy})_3]^{2+}$ glycerin data at 470 nm (a region of maximum difference in a and b). Figure 9 shows Arrhenius plots of the k_h values for three estimates of a , b , and c that are consistent with the maximum observed polarization at that wavelength.¹⁴ The k_h values are seen to be weakly dependent on the relative magnitude of the c component at all but the highest temperatures. The calculated barrier height (E_h) for the x - y depolarization phenomenon from Figure 9 is 4100 cm^{-1} .

The value of 4100 cm^{-1} seems high for a purely intramolecular barrier to exciton hopping and, in fact, is approximately equal to the viscosity "activation energy" for glycerin at these temperatures.⁷ Similarly, a linear Arrhenius plot is obtained for the ethanol/methanol data below 120 K. The slope of 1900 cm^{-1} is again characteristic of a (spherical) viscosity barrier for light alcohols. Above 120 K, the calculated k_h values appear to become nearly constant. However, uncertainties in the estimated D_R values lead to large uncertainties in the k_h values, and a method presenting the data in a form less dependent on D_R was sought.

The ratio of depolarization ratios (R_{pq}) at wavelengths at which the relative x and y contributions to the absorption oscillators are considerably different, although not entirely independent of D_R , assumes a very simple form for certain limiting conditions. If x - y depolarization dominates the photoselection spectrum ($k_h \gg D_R$, k_r), it follows from eq 8

$$R_{pq} = r_s(\lambda = p)/r_s(\lambda = q) = (a_p - c_p)/(a_q - c_q) \quad (14)$$

where the subscript on the absorption coefficient designates the wavelength. For the molecules investigated here, a is considerably larger than c , so R_{pq} is approximately unity. R_{pq} will reach another limiting value when k_h is effectively zero:

$$R_{pq} = (2a_p - b_p - c_p)/(2a_q - b_q - c_q) \quad (15)$$

Table I contains calculated R_{qr} for $p = 470 \text{ nm}$ and $q = 445 \text{ nm}$ for all the data presented in Figures 2–7. It is clear that for the glycerin and perhaps for the ethylene glycol/water data the former (eq 14) condition is met. In glycerin, $R_{pq} \approx 1$ well before polarization information is completely lost. In ethanol/methanol,

Table I. Ratios of r_s at 470 and 445 nm for $[\text{Ru}(\text{bpy})_3]^{2+}$ and 466 and 442 nm for $[\text{Ru}(\text{phen})_3]^{2+}$ as a Function of Temperature in the Indicated Solvents

T, K	$[\text{Ru}(\text{bpy})_3]^{2+}$				$[\text{Ru}(\text{phen})_3]^{2+}$	
	Et/Me ^a	Me/H ₂ O ^b	Etgly/ H ₂ O ^c	glycerin	Et/Me	glycerin
80					3.1	
90	4.1				3.1	
95	3.9					
100	3.7				3.0	
105	3.5					
110	3.1				2.7	
115	2.7					
120	2.2				2.0	
125	2.0					
130	2.0				1.7 ^d	
135	1.9					
140	2.8				2.1 ^d	
145	2.1					
150		1.8 ^d				
160		1.5 ^d	2.4			
170		1.2 ^d	2.0	2.9		
180		1.4 ^d	1.6			2.9
190			1.4	2.5		
200			1.2 ^d			2.5
210			1.1 ^d	2.0		2.3
215						2.2
220				1.9		2.0
225						1.9
230				1.7		1.7
235						1.4
240				1.4		1.3
245						1.1
250				1.3		1.1 ^d
260				1.1 ^d		1.1 ^d
270				1.0 ^d		
280				0.9 ^d		

^a 4:1 (v/v) ethanol/methanol. ^b 3:2 (w/w) methanol/water. ^c 1:1 (v/v) ethylene glycol/water. ^d Ratios taken from smoothed data.

both $[\text{Ru}(\text{phen})_3]^{2+}$ and $[\text{Ru}(\text{bpy})_3]^{2+}$ exhibit a nearly constant R_{pq} of approximately 2 across a wide temperature range which confirms that k_h is, as previously suspected, unchanging while, to account for the overall depolarization, D_R is increasing from a value which must be considerably less than k_r to one considerably greater.

The fact that the measured k_h attains a finite value in ethanol/methanol which is temperature independent (over a limited range) confirms that there are at least two processes responsible for the high polarization of these complexes. The initial (low temperature) depolarization event in ethanol/methanol, during which R_{pq} for $[\text{Ru}(\text{bpy})_3]^{2+}$ and $[\text{Ru}(\text{phen})_3]^{2+}$ decrease from nearly 4 to 2, is apparently a viscosity-dependent process (planar

depolarization) and may be attributed to solvent-induced ground-state distortion, perhaps, but not necessarily, associated with a glass transition. However, the maintenance of a nonunity R_{pq} at higher temperatures implies that another distortion process must be operating under these conditions. Since polarization structure is maintained in an environment in which Brownian rotation causes the nearly complete spherical depolarization of the luminescence, this distortion process is not solvent induced. *Only an intramolecular symmetry reduction phenomenon could be responsible for the latter polarization behavior.*

In glycerin the two depolarization processes cannot be distinguished. This does not seem unreasonable, since in glycerin the viscosity effect may be important at temperatures above which the intramolecular barrier to exciton hopping is overcome. Thus, the ethylene glycol/water or methanol/water data might be expected to provide a true k_h and measure of the barrier-to-exciton hopping. Unfortunately, an Arrhenius plot for these data gave a value of 3000 cm⁻¹, again implying a viscosity-dependent phenomenon. This too is not unexpected, since exciton hopping would involve a 120° shift of the excited-state "permanent" dipole, and strong solvent involvement (rearrangement) would be expected in such a change.²⁰

Conclusion

The temperature-dependent photoselection data presented above for $[\text{Ru}(\text{bpy})_3]^{2+}$ and $[\text{Ru}(\text{phen})_3]^{2+}$ provide strong evidence for an intramolecular excited-state localization phenomenon in these complexes. The photoselection data in 4:1 ethanol/methanol indicate that two nontrivial mechanisms are responsible for the high polarization observed in the strong charge-transfer region of the molecules' electronic absorption spectra, and one of these is active in an environment in which the molecule is strongly depolarized by rotational (spherical) motion. In glycerin, the effect of exciton localization cannot be unambiguously observed, since any polarization effects induced by the glassy environment are not relaxed until the temperature is so high that any intramolecular (exciton) effect is thermally overwhelmed. The E_h values measured for the water/alcohol solvents were also characteristic of a strong solvent interaction. The inability to separate the exciton-transfer barriers from the planar viscosity related barriers to solvent reorganization is not unexpected or unreasonable. It may, however, be possible to reduce or eliminate such solvent effects by studying derivatives of these complexes that are soluble in nonpolar liquids where solute-solvent dipole interactions are minimized. Studies of this type should enable measurement of the intramolecular barrier height and the hopping rate in these molecules.

Registry No. $\text{Ru}(\text{bpy})_3^{2+}$, 15158-62-0; $\text{Ru}(\text{phen})_3^{2+}$, 22873-66-1.

(20) Dellinger, B.; Kasha, M. *Chem. Phys. Lett.* **1976**, *38*, 9.